Rapid generation of microplastics and plastic-derived dissolved organic matter from food packaging films under simulated aging conditions

Environmental Science and Technology

Wang, L.; Gao, J.; Wu, W.M.; Luo, J.; Bank, M.S. et al

https://doi.org/10.1021/acs.est.4c05504

This publication is made publicly available in the institutional repository of Wageningen University and Research, under the terms of article 25fa of the Dutch Copyright Act, also known as the Amendment Taverne.

Article 25fa states that the author of a short scientific work funded either wholly or partially by Dutch public funds is entitled to make that work publicly available for no consideration following a reasonable period of time after the work was first published, provided that clear reference is made to the source of the first publication of the work.

This publication is distributed using the principles as determined in the Association of Universities in the Netherlands (VSNU) 'Article 25fa implementation' project. According to these principles research outputs of researchers employed by Dutch Universities that comply with the legal requirements of Article 25fa of the Dutch Copyright Act are distributed online and free of cost or other barriers in institutional repositories. Research outputs are distributed six months after their first online publication in the original published version and with proper attribution to the source of the original publication.

You are permitted to download and use the publication for personal purposes. All rights remain with the author(s) and / or copyright owner(s) of this work. Any use of the publication or parts of it other than authorised under article 25fa of the Dutch Copyright act is prohibited. Wageningen University & Research and the author(s) of this publication shall not be held responsible or liable for any damages resulting from your (re)use of this publication.

For questions regarding the public availability of this publication please contact openaccess.library@wur.nl

Environmental Science & Technology

pubs.acs.org/est

Article

Rapid Generation of Microplastics and Plastic-Derived Dissolved Organic Matter from Food Packaging Films under Simulated Aging Conditions

Liuwei Wang, Jing Gao, Wei-Min Wu, Jian Luo, Michael S. Bank, Albert A. Koelmans, John J. Boland, and Deyi Hou*

Cite This: https://doi.org/10.1021/acs.est.4c05504

Read Online

ACCESS | Metrics & More | Article Recommendations | Supporting Information

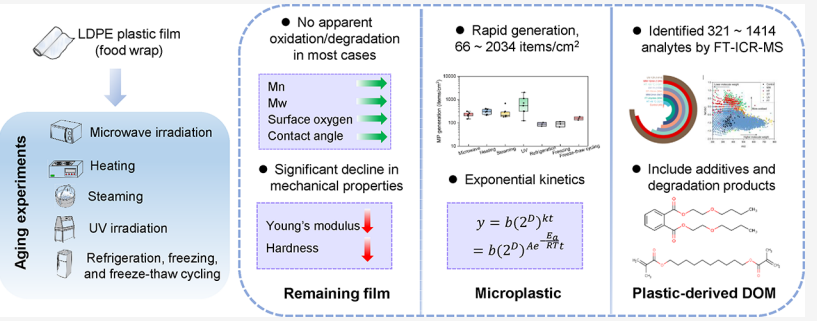

ABSTRACT: In this study, we show that low-density polyethylene films, a prevalent choice for food packaging in everyday life, generated high numbers of microplastics (MPs) and hundreds to thousands of plastic-derived dissolved organic matter (DOM) substances under simulated food preparation and storage conditions. Specifically, the plastic film generated 66−2034 MPs/cm^2 (size range 10−5000 μm) under simulated aging conditions involving microwave irradiation, heating, steaming, UV irradiation, refrigeration, freezing, and freeze−thaw cycling alongside contact with water, which were 15−453 times that of the control (plastic film immersed in water without aging). We also noticed a substantial release of plastic-derived DOM. Using ultrahigh-resolution mass spectrometry, we identified 321−1414 analytes with molecular weights ranging from 200 to 800 Da, representing plastic-derived DOM containing C, H, and O. The DOM substances included both degradation products of polyethylene (including oxidized forms of oligomers) and toxic plastic additives. Interestingly, although no apparent oxidation was observed for the plastic film under aging conditions, plastic-derived DOM was more oxidized (average O/C increased by 27−46%) following aging with a higher state of carbon saturation and higher polarity. These findings highlight the future need to assess risks associated with MP and DOM release from plastic wraps.

KEYWORDS: *microplastic, FT-ICR-MS, aging, polyethylene, food packaging*

Downloaded via WAGENINGEN UNIV & RESEARCH on November 5, 2024 at 09:03:10 (UTC).
See https://pubs.acs.org/sharingguidelines for options on how to legitimately share published articles.

1. INTRODUCTION

Plastic polymers have been widely used since the 1950s, with global production reaching 400.3 million tonnes by 2022.[1] Among the various applications of plastics, the largest market is packaging, which accounts for 44% of all plastic production on a global scale; furthermore, over 50% of the plastic packaging produced is used for food packaging.[1−3] Among synthetic plastic polymers available, polyolefins, including polyethylene (PE) and polypropylene (PP), are widely used in various aspects of food preparation and storage conditions.[1,4,5] For example, PP is widely used in the manufacture of containers and bottles,[6,7] and low-density polyethylene (LDPE) ranks as the most commonly used polymer for packaging films.[2,8]

While it is widely recognized that plastic packaging effectively safeguards food from environmental contamination, the direct human health risks associated with these materials used for food preparation and storage have been raised.[9−11] On one hand, the aging (weathering) of plastic polymers throughout the life cycle of packaging leads to the generation of microplastics (MPs, <5 mm) during use.[12,13] It has been frequently reported that plastic products have the potential to generate MPs under everyday use conditions, including infant feeding bottles (14,600−4,550,000 particles/capita/day),[6] breastmilk storage bags (0.61−0.89 mg/capita/day),[14] tea bags (around 11.6 billion particles/bag/cup),[15] mineral water

Received: June 1, 2024
Revised: September 28, 2024
Accepted: October 15, 2024

ACS Publications © XXXX American Chemical Society

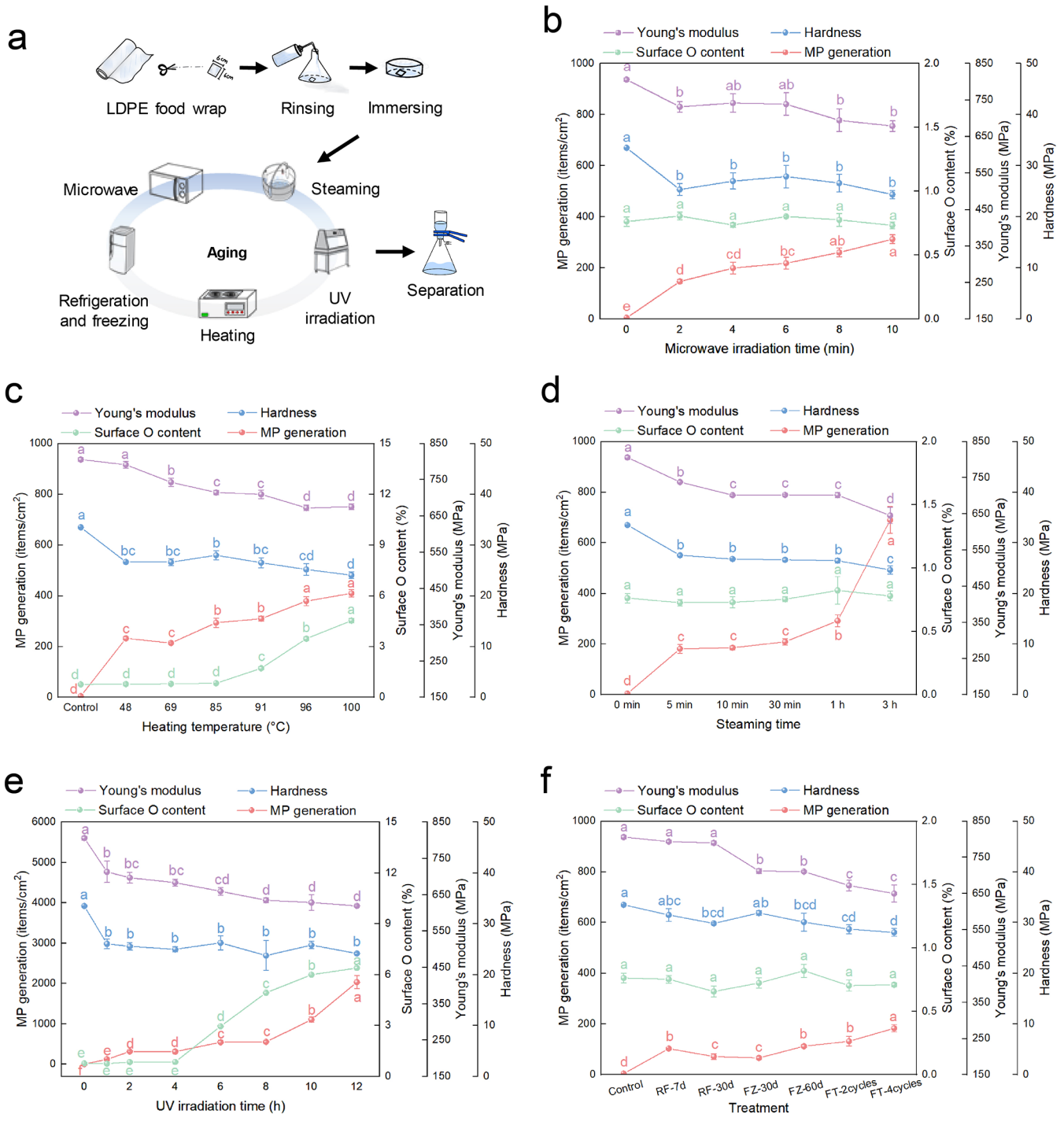

Figure 1. (a) Schematic diagram of the aging experiments. (b–f) MP generation, changes in Young's modulus, hardness, and surface oxygen content of plastic films following different treatments, including (b) microwave irradiation, (c) heating, (d) steaming, (e) UV irradiation, and (f) refrigeration (RF), freezing (FZ), and freeze–thaw cycling (FT).

bottles (up to 5907 ng/L),[16] and food containers (up to 4.22 million particles/cm^2).[17] Plastic food packaging materials are a significant source of human intake of MPs. For adults, estimated MP (with sizes ranging from 1 μm to 5 mm) intake has been reported to be up to 322,295 particles per year through inhalation and food consumption.[18] Furthermore, MPs generated from the everyday use of these plastic products can also enter aquatic and terrestrial environments, thus raising ecological concerns.[19,20]

On the other hand, submicron-sized organic substances (<1 μm) released from plastic products have also attracted much attention.[17,21−23] Nevertheless, our knowledge of these tiny substances remains very limited compared to micron-sized MPs larger than 1 μm, partly due to analytical challenges,[24,25] and many discrepancies and inconsistencies exist in this field. For instance, traditional optical and spectroscopic approaches have significant difficulties in quantifying submicron colloidal particles and soluble substances in most cases.[21,26] The

https://doi.org/10.1021/acs.est.4c05504
Environ. Sci. Technol. XXXX, XXX, XXX−XXX

submicron-sized substances detected are usually described using the umbrella term nanoplastics (NPs) in many environmental studies;[27−29] however, this simplicity may not accurately describe the complicated nature of these substances, which are mixtures of NPs (with more than 40 repeating units), oligomers (with less than 40 repeating units), monomers, degradation products, and plastic additives in the context of polymer science.[12,30−32] Despite these inconsistencies, it is generally acknowledged that the bioavailability and toxicity of these submicron substances are much higher than those of micron-sized MPs, primarily due to their smaller sizes and lower molecular weights.[33−35] Among these submicron-sized substances, the even smaller proportion is referred to as plastic-derived dissolved organic matter (DOM), sharing the same size cutoff value as the natural DOM (usually below 0.45 or 0.22 μm).[36−38] It was also estimated that plastic-derived DOM contributes significantly to the DOM pool in the natural environment. For instance, approximately 23,600 t of carbon as plastic-derived DOM is leached to the ocean annually, making up to 10% of the total DOM pool in the surface microlayer (namely, the top 40 μm) of the ocean water column.[36]

It should be acknowledged that the human health risks and ecological implications associated with specific DOM, as well as its bioavailability and degradability in the environment, are related to its molecular composition and associated properties such as molecular weight, hydrophilicity, polarity, and aromaticity. For instance, low-molecular-weight (<350 Da) acids from the plastic-derived DOM pool were reported to contribute more to the formation of the disinfection byproduct trihalomethanes compared to high-molecular-weight DOM substances.[39] Phenol/protein-like moieties from the plastic-derived DOM pool were indicative of bisphenol A from the plastic polymer.[40] Another study found that protein-like DOM derived from plastic had high microbial bioavailability, which increased marine bacterial activity.[41] Providing a basic understanding of the molecular-level composition of plastic-derived DOM is, therefore, a topic worthy of investigation. With the development of ultrahigh-resolution Fourier transform ion cyclotron resonance mass spectrometry (FT-ICR-MS), it is now possible to provide high-throughput, molecular-level characterization of DOM in natural environmental samples, including soil and water bodies.[42−44] Typically, hundreds to thousands of DOM analytes are simultaneously identified with high mass accuracy.[45,46] Several recent studies have also proposed that the same method can be extrapolated to provide a molecular-level, nontargeted analysis of plastic-derived DOM.[37,47−49] Using the negative-ion electrospray ionization (ESI) method, organic substances released from bulk plastic materials, with diverse analytes containing carbon (C), hydrogen (H), and oxygen (O), can be accurately characterized.[37,47,48] For instance, Stubbins et al.[37] identified 319−705 analytes in DOM released from PE, PP, and expanded polystyrene (PS) in simulated sunlit seawater, whose average H/C values decreased by 10−15% compared to the bulk polymer, showing signs of chain-scission and photo-oxidation.[37] Plastic additives, oxidized oligomers, and other aging-induced degradation products can be simultaneously analyzed from such molecular-level characterization,[37,47,48] which can substantially enhance our understanding of the aging and degradation processes of plastic polymers and provide a fundamental molecular understanding prior to the precise risk assessment of plastic-associated substances.

In this study, we explored the characteristics of MP and plastic-derived DOM generation from commercially available LDPE food wrap, which is widely used in kitchens around the world as a primary representative of plastic food packaging materials. We conducted a series of aging experiments to simulate everyday food preparation and storage conditions of food wraps, including microwave irradiation, steaming, heating, refrigeration, freezing, and freeze−thaw cycling. Additionally, we exposed the materials to UV irradiation to mimic exposure to sunlight. We examined the extent of plastic film degradation, physicochemical changes of the plastic film, MP generation characteristics, and plastic-derived DOM generation characteristics. The findings from this study provide a molecular-level understanding of polymer aging characteristics under everyday use and storage conditions, which are useful for future human health risk assessments of plastic food packaging materials.

2. MATERIALS AND METHODS

2.1. Plastic Food Wrap Preparation. Commercially available food wrap made from LDPE with an average thickness of 8.4 ± 0.2 μm (mean and standard error values, $N = 6$) was utilized for this study. The purity of the food wrap was determined to be 99.5% by GC−MS, following Soxhlet extraction with chloroform (1 g of plastic with 100 mL of solvent, extracted at 85 °C for 8 h). To prepare the LDPE plastic films for experimentation, samples were cut into square pieces measuring 6 cm × 6 cm. Subsequently, the pieces were rinsed three times using ultrapure water (resistivity of 18.2 MΩ·cm, produced with a final filter of 0.2 μm) and left to air-dry (∼4 h). Each square piece was then placed in a glass Petri dish (10 cm in diameter and 2 cm in height).

2.2. Aging Experiments Simulating Food Preparation and Storage Conditions. A series of aging experiments were conducted to simulate various scenarios representing different everyday uses and storage conditions of LDPE food wraps in contact with food that contains water (Figure 1a). UV irradiation experiments were also conducted as an acceleration of sunlight-induced aging of plastic wrap. 40 mL of ultrapure water was added to a Petri dish containing one piece of plastic film in each experiment. It is important to note that in these experiments, the volume of water may change due to temperature changes. The water content was not kept at a steady value in these experiments to better simulate everyday use conditions because evaporation and condensation of water also occur during daily use of food wraps. The changes in water volume did not affect MP and DOM quantification because all remaining water and the rinsing water were combined prior to analysis and MP and DOM concentrations were reported relative to the plastic film (namely, items/cm^2 and μg/cm^2). In this study, one piece of plastic film covered an area of 36 cm^2.

Microwave irradiation was conducted by putting water-immersed food wrap into a household microwave oven (M1-L213B, Midea, China) (2450 MHz) with an operating power of 119 W for specific durations of 2, 4, 6, 8, and 10 min. The selected times were chosen to mimic the use of a microwave oven for liquid (e.g., milk, infant formula) or food (e.g., meat, vegetables, precooked meals) preparation. The temperature of the soaking water was measured directly after irradiation, yielding values of 48, 69, 85, 91, and 96 °C, respectively.

For the heating experiments, the immersed food wrap was placed in a thermostatic water bath (HH-4, Kexi Instrument, China) for 30 min at set temperatures of 48, 69, 85, 91, 96, and 100 °C. This aging treatment simulates the use of warm or hot

https://doi.org/10.1021/acs.est.4c05504
Environ. Sci. Technol. XXXX, XXX, XXX−XXX

water for liquid (e.g., milk, infant formula) or food preparation (e.g., precooked meals).

For steaming experiments, the immersed food wrap was placed in a cooking steamer (ZN28YC808-130, Supor, China) containing boiling water. The setup was exposed to water vapor for durations of 5 min, 10 min, 30 min, 1 h, and 3 h. This aging process simulates the use of steaming to prepare liquids (e.g., milk and infant formula) for a relatively short time or foods (e.g., meat and staple food) for a longer time.

For long-term refrigeration scenarios, the immersed food wrap was stored in a refrigerator (BCD-470WDPG, Haier, China) for 7 and 30 days at a temperature of 4 °C. Similarly, for long-term freezing conditions, the immersed food wrap was stored for 30 and 60 days at a temperature of −20 °C. Freeze−thaw cycling was performed by putting the immersed food wrap in the freezer set at −20 °C for 24 h, followed by thawing at room temperature of 25 °C for an additional 24 h. This freeze−thaw cycle was repeated 2 and 4 times for subsequent testing. These treatments simulate different storage conditions of food in refrigerators.

UV irradiation experiments involved exposing the immersed food wrap to an aging chamber equipped with a UVA 340 (type 1A) UV lamp with maximum emission at 340 nm, following the ISO 4892-3:2016 standard.[50] The exposure durations were 1, 2, 4, 6, 8, 10, and 12 h. This specific UV lamp type is recommended by ISO for simulating UV irradiation similar to sunlight.[50] The lamp had an irradiance of 100 W/m^2, and the irradiation process was conducted at room temperature (25 °C). The temperature at the surface of the food wrap remained below 30 °C throughout the experiment. It is widely acknowledged that UV is an important process leading to polyolefin polymer degradation.[51,52] Therefore, this aging experiment simulates a worst-case scenario of LDPE aging, which may also occur (albeit in fewer cases) during the use and storage conditions of LDPE food wraps when exposed to sunlight. Additionally, we calculated an equivalent UV irradiation time on Earth's land surface for specific irradiation periods using our previously established method,[53] assuming an annual UV radiation of 179 MJ/m^2 at the land surface.[54] In this case, 12 h of chamber irradiation is equivalent to 8.8 days of exposure.

Following each treatment, plastic films were separated from water and rinsed three times using ultrapure water. To establish a control group, untreated food wrap was immersed in 40 mL of ultrapure water for 1 h at room temperature and then rinsed three times directly using ultrapure water. The rinsing water was combined with the original soaking water, and any MPs present were isolated and collected by using stainless steel filter with a pore size of 10 μm. Note that any large particles >5000 μm were removed using a stainless steel mesh. Subsequently, the collected MPs were transferred to clean, dry glass Petri dishes for further analyses.

Additionally, we investigated whether the contacting liquid affected the number of MPs generated. Plastic film pieces were soaked in 40 mL of 3% acetic acid as a food simulant representing acidic food matrices,[17,55] as well as in 40 mL of commercially available whole milk, and 40 mL of commercially available infant formula (Stage 1, from birth to 6 months) prepared according to the manufacturer's guidelines (15 g of powder dissolved in 100 mL of water). The immersed food wrap was then subjected to microwave irradiation for 2 min or steaming for 5 min, representing frequently used parameters for milk, infant formula, and food preparation, and subsequently subjected to MP separation using the same methods mentioned above.

2.3. MP Characterization and Modeling. The collected MP particles were stained with Nile Red following the methods described by Maes et al.[56] and Wang et al.[57] Laser confocal scanning microscopy (FV 3000RS, Olympus, Japan) was subsequently used to identify the stained samples.[58,59] MPs with a size range of 10−5000 μm were assessed in this study. Quantitative measurements were conducted using ImageJ software (https://imagej.nih.gov/ij/). The average particle size was determined using Feret's diameter.[60,61] Furthermore, the size distribution of MPs after various aging treatments was analyzed in accordance with the procedure described by Wang et al.[57] Specifically, the cumulative size distribution function of MPs was depicted using the conditional fragmentation model (eq 1):

$$F(x) = 1 - e^{-\lambda x^{\alpha}} \quad (x \geq 0) \tag{1}$$

where λ and α refer to the range parameter and fragmentation parameter, respectively.[57] Detailed size distribution modeling information is provided in Text S1 and Table S1. The size distribution data are plotted in Figure S1.

Besides, we derived an exponential model depicting MP generation kinetics from aging treatments. The detailed derivation of the model, along with relevant assumptions, can be found in Text S2. The model was also further validated using literature data following the literature search protocol mentioned in Text S3. A graphical representation of the literature searching and screening methodology is provided in Figure S2. The modeling results obtained from the analysis are presented in Table S2. The fragmentation dimension was determined to be 2 (Table S3).

2.4. Physical and Chemical Characterizations of the Remaining Plastic Film. Young's modulus and the hardness of the pristine and aged food wraps were measured using a nanoindenter (G200, Keysight Technologies, USA) with a diamond Berkovich tip.[62,63] The surface oxidation characteristics of the pristine and aged plastic films were first examined using Fourier transform infrared (FTIR) spectroscopy (Nicolet iS50, Thermofisher, USA) with a resolution of 4 cm^{-1}, covering the wavenumber range from 4000 to 400 cm^{-1}. The obtained FTIR spectra also underwent 2D-COS analysis[64] to obtain comprehensive information regarding the aging process. Theoretical details can be found in Text S4. Second, X-ray photoelectron spectroscopy (XPS) (250 Xi, Thermofisher, USA) was also employed to investigate surface oxidation and quantitatively calculate the surface oxygen content (in atomic ratio). The C 1s spectra were fitted using CasaXPS software using the Gaussian−Lorentzian function following background subtraction using the Shirley method.[65] In addition, we employed a Raman spectrometer (LabRAM HR Evolution, HORIBA) equipped with a 532 nm laser operating at an output power of 100 mW to gather Raman spectra of the plastic films.[66,67] To detect the Raman signals, we utilized a charge-coupled device detector (Horiba Synapse), which was coupled to the laser. In addition to these spectroscopic characterizations, the contact angle of the plastic film in ultrapure water was measured using a Dataphysics OCA25 system. Furthermore, the surface morphologies of the plastic films were characterized by field-emission scanning electron microscopy (GEMINISEM 500, ZEISS, Germany).

2.5. Polymer Degradation Characterization of the Remaining Plastic Film. To examine the degradation

https://doi.org/10.1021/acs.est.4c05504
Environ. Sci. Technol. XXXX, XXX, XXX−XXX

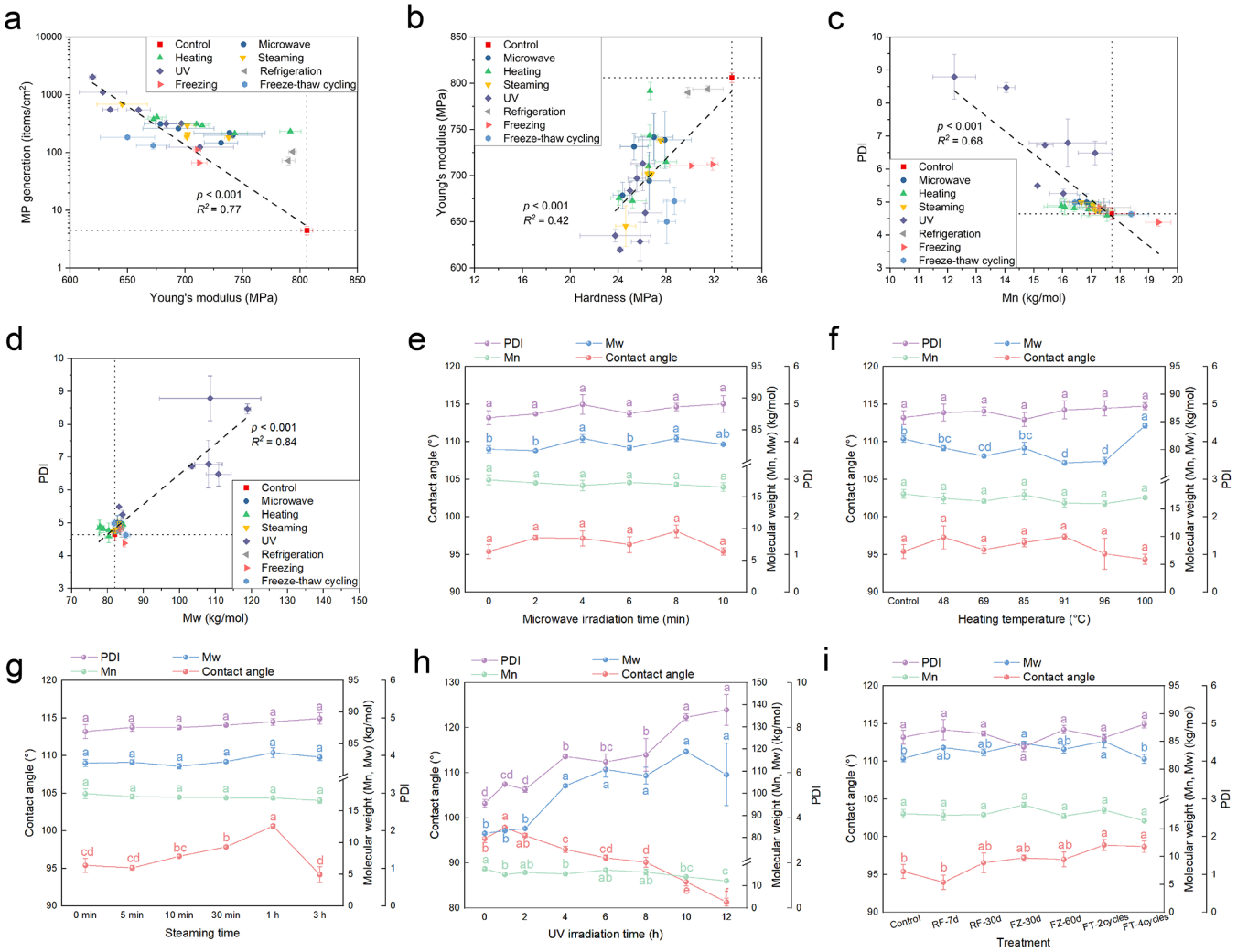

Figure 2. (a) Exponential relationship between Young's modulus of the remaining plastic film and the number of MPs generated. (b) Linear correlation between hardness and Young's modulus of the remaining plastic film. (c) Linear correlation between Mn and PDI of the remaining plastic film. (d) Linear correlation between Mw and PDI of the remaining plastic film. (e–i) Changes in PDI, Mw, Mn, and contact angles of the remaining plastic film following different treatments, including (e) microwave irradiation, (f) heating, (g) steaming, (h) UV irradiation, and (i) refrigeration (RF), freezing (FZ), and freeze–thaw cycling (FT).

characteristics of the plastic films, the samples were dissolved in 1,2,4-trichlorobenzene and analyzed with gel permeation chromatography (GPC) using the SECurity GPC system (Infinity II High Temperature GPC System, Agilent Technologies, USA). The column setup encompassed a guard column (PLgel 10 μm Guard, 5 × 0.75 cm) along with two separation columns (PLgel 10 μm MIXED-B, 30 × 0.75 cm). The separation of molecules was accomplished by utilizing an eluent of 1,2,4-trichlorobenzene containing 0.3 g/L butylated hydroxytoluene, while the calibration was carried out employing narrowly distributed PS standards.[68,69] A sample volume of 1 μL (1 mg/mL) was measured at a flow rate of 1 mL/min and a temperature of 150 °C.[70−72] Meanings of key parameters from GPC analysis are provided in Text S5.

2.6. Plastic-Derived DOM Characterization with FT-ICR-MS. DOM generated from nine representative treatments with the plastic film immersed in water, including the control, microwave irradiation for 2 and 10 min, heating at 48 and 100 °C, steaming for 10 min, UV irradiation for 1 and 12 h, and freeze–thaw cycling for 2 rounds, underwent further characterizations. A total of 36 replicates (each containing one piece of plastic film and 40 mL of water) were set up for each treatment to generate an adequate mass of DOM for FT-ICR-MS analysis. Following aging experiments as described in Section 2.2, the remaining liquid and the rinsing solution from these replicates were combined and filtered through a 0.45 μm glass fiber membrane.[48,49] The dissolved organic carbon (DOC) content of the liquids was measured using a TOC analyzer (TOC-L, Shimadzu Corporation, Japan).

An FT-ICR-MS (Solarix, Bruker, USA) equipped with a 15 T superconducting magnet was employed for molecular-level characterization of DOM. 1 L of acidified combined liquid samples (adjusted to pH 2 using HPLC-grade HCl) underwent an established method for plastic-derived DOM purification, involving solid-phase extraction with a PPL cartridge at a flow rate of 10 mL/min, and elution using 6 mL of methanol.[37,47] The samples were then injected into the FT-ICR-MS operating in the negative-ion ESI mode at the rate of 2 μL/min to characterize CHO-containing compounds.[47] A total of 300 transient scans were coadded to increase the signal-to-noise (S/N) ratio. The mass spectra were externally calibrated with 10 mmol/L sodium formate and internally recalibrated with

https://doi.org/10.1021/acs.est.4c05504
Environ. Sci. Technol. XXXX, XXX, XXX−XXX

the Suwannee River Fulvic Acid standard, achieving a mass error of <0.1 ppm.[49] The isotopic spacing pattern suggested that all ions were singly charged. Experimental data were processed using the following criteria set by previous studies using FT-ICR-MS for DOM characterization:[47,49,73] 200 < m/z [the ratio of mass (m) to its charge (z)] < 800, S/N > 6, 0 < O/C < 1.2, 0.3 < H/C < 2.2. Several key indicators of molecular compositions were calculated, including O/C, H/C, normal oxidation state of carbon (NOSC),[74] double-bond equivalent minus oxygen (DBE-O),[75] and modified aromaticity index (AImod).[76] Calculation methods and meanings of these parameters are provided in Text S6.

The most abundant formulas were further compared with existing databases of plastic additives and chemicals associated with plastic packaging, including the Database of Chemicals associated with Plastic Packaging (CPPdb),[77] the Plastic Additives Initiative Mapping Exercise by European Chemical Agency (ECHA),[78] the Food Contact Chemicals database (FCCdb) (version 5),[79] and the database for extractables and leachates from food contact materials developed by Song et al.[80] If a formula was found in any of these databases, then it was marked as a "plastic additive." It is worth noting that this term encompasses both intentionally added additives and nonintentionally added substances. Formulas not present in these databases were further searched in online chemical databases, including the REACH database (https://comptox.epa.gov/dashboard/chemical-lists/reach2017), and PubChem (https://pubchem.ncbi.nlm.nih.gov/).

2.7. Quality Control and Statistical Analyses. Information on quality control measures and statistical analyses is provided in Text S7.

3. RESULTS AND DISCUSSION

3.1. Rapid Generation of MPs during Simulated Food Preparation and Storage Conditions. The food wrap generated MPs at a rapid rate under different aging treatments (Figure 1b−f). Even at the initial stage of each aging treatment, significantly higher numbers of MPs were generated compared with the control (Figure 1b−f). After only 2 min of microwave irradiation, the food wrap produced 147 MPs/cm^2, which was 32.7 times that of the control without irradiation, and the amount gradually increased to 313 MPs/cm^2 at 10 min (69.6 times that of the control) (Figure 2b). When plastic food wrap was subjected to various heating temperatures for 30 min, it generated between 214 and 410 MPs/cm^2 (47.6−91.3 times that of the control) (Figure 2c). Steaming for 5 min to 3 h yielded 181−690 MPs/cm^2 (40.4−154 times that of the control) (Figure 2d). Accelerated UV irradiation substantially increased the MP generation, with counts rising from 123 MPs/cm^2 at 1 h (equivalent to 0.7 days of sunlight exposure) to 2034 MPs/cm^2 at 12 h (equivalent to 8.8 days of sunlight exposure), reaching 27.5−453 times that of the control, respectively (Figure 2e). Refrigeration for 7 and 30 days led to the generation of 103 and 72 MPs/cm^2, respectively (23.0 and 16.0 times that of the control) (Figure 2f). Freezing for 30 and 60 days resulted in the generation of 66 and 112 MPs/cm^2, respectively (14.8 and 25.1 times that of the control) (Figure 2f). Furthermore, when subjected to multiple freeze−thaw cycles at 2 and 4 times, the food wrap produced 132 and 183 MPs/cm^2, respectively (29.4 and 40.8 times that of the control) (Figure 2f). Furthermore, it was observed that food wrap in contact with 3% acetic acid, representing acidic food matrices, released a higher number of MPs compared to the food wrap in water under microwave irradiation (p < 0.05) and steaming (p > 0.05). The number of MPs released from food wrap immersed in whole milk and infant formula showed no significant difference (p > 0.05) (Figure S5). The food wrap generated 171, 132, and 134 MPs/cm^2 in 3% acetic acid, whole milk, and infant formula, respectively, after microwave irradiation for 2 min (Figure S5). The MP generation values were 208, 160, and 163 MPs/cm^2 in 3% acetic acid, whole milk, and infant formula, respectively, following steaming for 5 min (Figure S5).

The size distribution of MPs can be well described using the conditional fragmentation model, whose parameters are provided in Table S1. Over 50% of the identified MP particles fell below 20 μm under most treatments (Table S1). The kinetic model we developed fitted well with the experimental data (Figure S6). To validate the applicability of this exponential generation model, we utilized previously published MP generation data with various polymer types, aging processes, and durations. The model successfully depicted these data, with the fit being statistically significant (p < 0.05) in most cases (Figure S6, Table S2). We further compared the fragmentation rate constants from exponential model fitting (Figure S6f,g). The MP generation rate from LDPE aging in this study (including UV irradiation and steaming) exceeded the rate constants observed in landfill environments,[81] agricultural soils,[82] maritime rope abrasion,[83] and ozone oxidation,[84] and they were comparable to MP generation rates reported from sea swash zones[85] (Figure S6f,g, Table S2). Notably, a wide range of fragmentation rate constants were observed in studies employing mechanical abrasion and UV irradiation for MP generation. UV irradiation and steaming exhibited a much higher efficacy in MP generation when combined with water soaking, surpassing the impact of irradiating soil with buried plastic debris (Figure S6f). Moreover, the rate constants for specific polymer types exhibited high variability spanning several orders of magnitude (Figure S6g). However, on average, the rate constants for LDPE polymers exceeded those of other polymers, including high-density polyethylene, PP, PS, polyvinyl chloride, and polybutylene succinate, suggesting that LDPE has greater susceptibility to fragmentation (Figure S6g).

3.2. Physical and Chemical Changes of the Remaining Plastic Film. MP generation from various treatments was accompanied by a significant decline in Young's modulus and hardness of the remaining plastic film but without a significant increase in surface oxygen content in most cases (Figure 1). Significant changes in mechanical properties were observed during the aging process for microwave irradiation, steaming, refrigeration, freezing, and freeze−thaw cycling treatments, with no observed significant change in the surface oxygen content (Figure 1). The level of surface oxygen consistently remained below 1% for these treatments (Figure 1). Only for certain treatments, including heating temperatures exceeding 91 °C and UV irradiation lasting over 6 h, did chemical oxidation of the food wrap become statistically significant (Figure 1).

The decline in mechanical properties occurred since the initial stages of the aging treatments (Figure 1). Further decreasing trends in both values were observed with increasing aging time or temperature for different treatments (Figure 1). Notably, the relationship between Young's modulus and the number of generated MPs followed an exponential trend—the lower the Young's modulus, the higher the number of MPs

https://doi.org/10.1021/acs.est.4c05504
Environ. Sci. Technol. XXXX, XXX, XXX−XXX

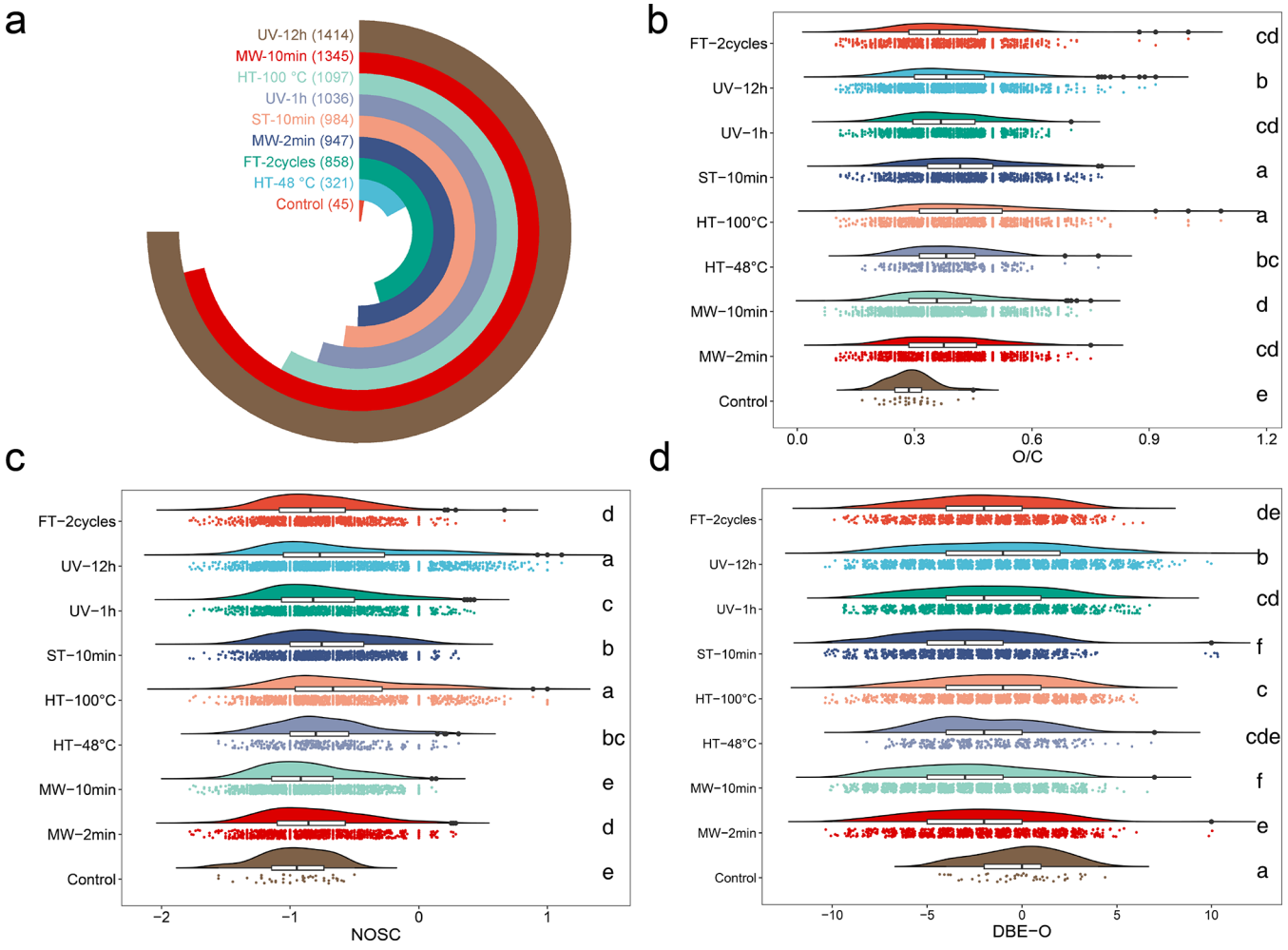

Figure 3. (a) Number of identified DOM analytes containing C, H, and O following different treatments. (b–d) Distribution of (b) O/C, (c) NOSC, and (d) DBE-O values of DOM substances following different treatments. Abbreviations: MW, microwave irradiation; HT, heating; ST, steaming; UV, UV irradiation; and FT, freeze–thaw cycling.

generated (Figure 2a). A linear correlation was also found between hardness and Young's modulus (Figure 2b). Direct evidence of physical deterioration was observed for all aging treatments, with the aged food wraps exhibiting crazing (i.e., a yielding mechanism in polymers characterized by the formation of a fine network of microvoids and fibril) and cracking (Figure S7).[86]

Multiple lines of evidence from FTIR spectra, Raman spectra, XPS spectra, and contact angle measurements suggested that chemical oxidation was not the dominant change for the remaining plastic film in most treatments as compared with the aforementioned changes in mechanical properties. FTIR raw spectra did not reveal any oxygen-containing functional groups for any of the treatments (Figure S8). Nevertheless, 2D-COS maps of FTIR spectra revealed mild oxidation for UV treatments (Figure S9). Similarly, identifiable changes were not observed in the Raman spectra (Figure S10). Nevertheless, XPS C 1s spectra of specific treatment groups indicated the generation of oxygen-containing functional groups, notably in cases of heating at 96 and 100 °C, as well as UV irradiation for over 6 h (Figures S11–S13). The contact angle of the remaining food wraps did not decrease following most aging processes, with the exception of UV irradiation, further suggesting that oxygen-containing functional groups were not introduced due to surface oxidation in these cases[87,88] (Figure 2).

3.3. Polymer Degradation Characteristics of the Residual Plastic Film. An insignificant change in the number-average molecular weight (Mn) and polydispersity index (PDI) was observed throughout the entire heating, steaming, microwave irradiation, refrigeration, freezing, and freeze–thaw cycling processes ($p > 0.05$), suggesting negligible polymer degradation of the residual plastic film[89−91] (Figure 2). These findings are consistent with previous theories on polyolefin degradation, which suggest that everyday use and storage conditions, in the absence of sunlight irradiation, result in only mild aging of plastic polymers and are unlikely to cause significant degradation of the bulk plastic film.[51,92] The weight-average molecular weight (Mw) followed these aging processes fluctuated, suggesting a higher sensitivity to aging.

For UV irradiation, fluctuations in Mn were observed, and a significant decrease in Mn occurred for some samples, possibly due to chain-scission triggered by Norrish reactions[51,87,93] (Figure 2). A significant increase in Mw during UV irradiation also suggested the possible presence of cross-links during polymer degradation[51,94] (Figure 2). Lower Mn and Mw values were correlated with higher PDI, suggesting an increased polymer composition heterogeneity following UV irradiation (Figure 2c,d).[51,95] The elevation of Mw and PDI

https://doi.org/10.1021/acs.est.4c05504
Environ. Sci. Technol. XXXX, XXX, XXX−XXX

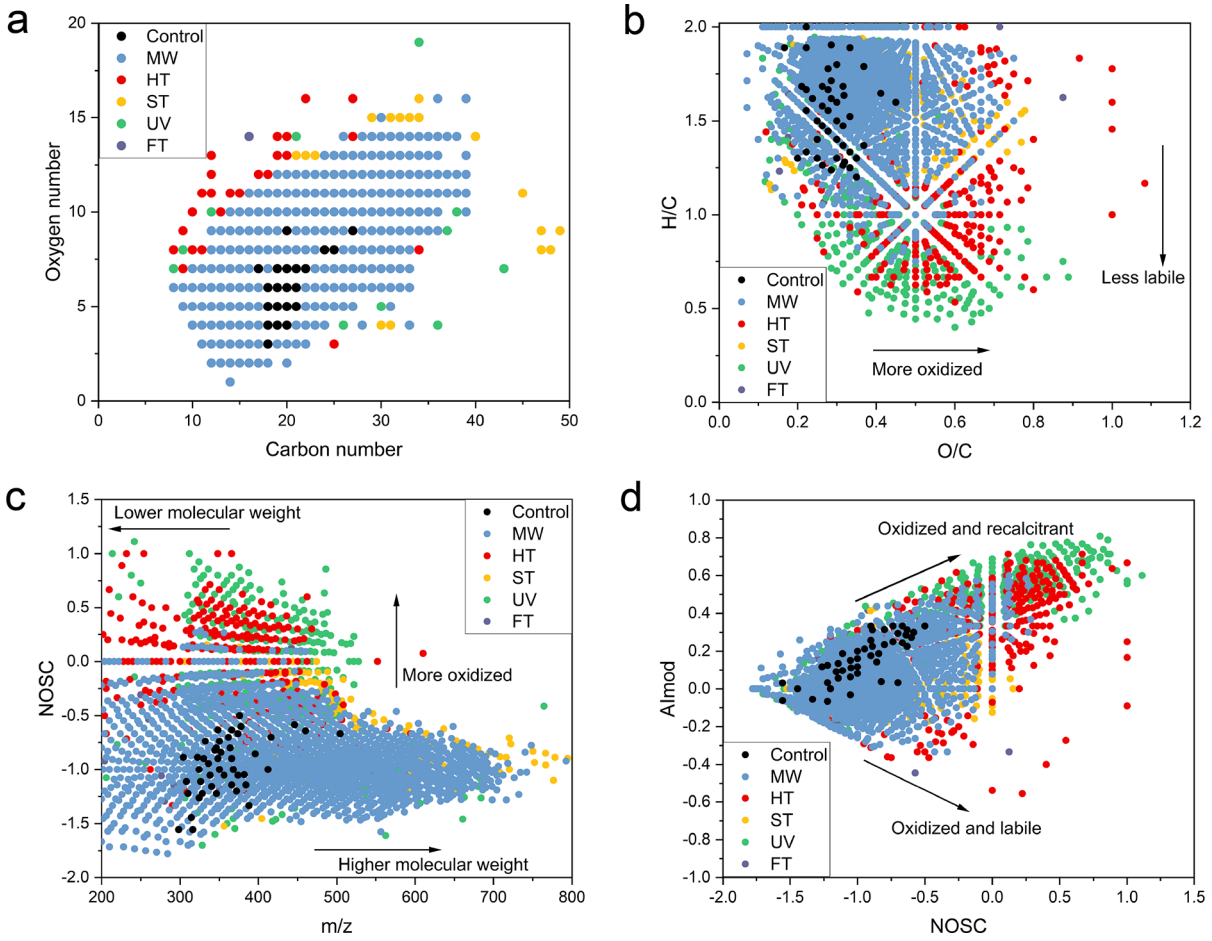

Figure 4. (a) Changes in carbon number vs oxygen number of the identified DOM analytes following aging. (b) Van Krevelen diagram showing changes in O/C and H/C values of the identified DOM analytes following aging. (c) Changes in m/z vs NOSC values of the identified DOM analytes following aging. (d) Changes in NOSC vs AImod values of the identified DOM analytes following aging. Abbreviations: MW, microwave irradiation; HT, heating; ST, steaming; UV, UV irradiation; FT, freeze−thaw cycling.

under UV irradiation are also possible signs of long-chain branching.[51,96] It is also important to note that sunlight cannot initiate the degradation of pure polyolefin because the UV light reaching the Earth's land surface falls between 290 and 400 nm, and its transferred energy is too low to react with the paraffinic bonds.[51] Instead, it is the unsaturated sites, either introduced during the polymerization process or by intentionally or nonintentionally added additives, that initiate the polymer chain-scission processes.[51,89]

3.4. Release and Molecular Compositions of Plastic-Derived DOM. The DOC concentration of the control was 0.026 ± 0.001 μg-C/cm^2 (equivalent to 0.033 ± 0.002 mg-C/g plastic) (Figure S14). Aging significantly enhanced the release of DOC ($p < 0.05$), resulting in DOC concentrations ranging from 0.173 ± 0.004 μg-C/cm^2 (0.224 ± 0.005 mg-C/g) to 0.896 ± 0.008 μg-C/cm^2 (1.159 ± 0.010 mg-C/g), which were 6.8−35 times that of the control (Figure S14). These concentrations were comparable to previously reported data on DOC release following plastic aging.[37,38,47]

A total of 45 DOM analytes containing CHO were identified from the control group without aging (Figure 3a), among which 40 analytes were observed across all nine samples subjected to FT-ICR-MS characterization (Figure S15). These most frequently observed analytes were likely to be either plastic additives or degradation products (accounting for 25 and 75% of the analytes, respectively) (Table S5). Certain analytes exhibited a long straight chain with oxidation (for instance, 1,10-decanediol dimethacrylate; 9,10-dihydroxyoctadecanoic acid; 4-[3-(dodecanoyloxy)-2-hydroxypropoxy]-4-oxobutanoic acid), which were possibly the oxidized forms of PE oligomers (Table S5).

A total of 321−1414 analytes were identified following different aging processes, which were 7.1−31.4 times that of the control (Figure 4a). It is also notable that a higher number of analytes were identified compared to the control, even at the initial stage of aging (Figure 4a). A significant positive correlation was observed between the number of DOM analytes identified and the DOC content ($p < 0.001$, R^2 = 0.96) (Figure S14). DOM released following different aging processes, including microwave irradiation for 2 or 10 min, heating at 48 or 100 °C, steaming for 10 min, UV irradiation for 1 or 12 h, and freeze−thaw cycling for 2 rounds, consistently exhibited significantly higher average O/C values, higher NOSC, and lower DBE-O ($p < 0.05$) (Figure 3b−d). These findings suggest that DOM following aging became more oxidized, had higher polarity, and a higher state of carbon saturation.[47,74,75] It is noteworthy that this phenomenon was in stark contrast to changes in the oxygen content in the bulk plastic film following aging. It could be that plastic-derived DOM is more susceptible to aging and more easily oxidized under simulated everyday use and storage conditions. It could also be that the aged and more oxidized portions of the plastic

https://doi.org/10.1021/acs.est.4c05504
Environ. Sci. Technol. XXXX, XXX, XXX−XXX

polymer are more likely to be released into water. Additionally, the higher specific surface area of smaller DOM particles compared to MPs may also have contributed to this phenomenon.

The molecular weights of the DOM had wider ranges following aging compared with the control (Figure 4ac), and the average m/z values increased for all groups following aging (Table S14). The van Krevelen diagram (explained in detail in Text S6) also showed a wider distribution of H/C and O/C values of the DOM (Figure 4b). The average H/C values for DOM for microwave irradiation, steaming, and freeze−thaw cycling slightly increased compared to the control, suggesting higher biodegradability, while those for heating and UV irradiation slightly decreased, rendering lower biodegradability.[97] The formation of more recalcitrant substances under heating and UV irradiation could be attributed to enhanced cross-linking reactions, leading to the generation of cross-linked molecules with higher molecular weights.[51,94] Results from GPC supported this hypothesis, as the Mw for certain treatments, including heating at 100 °C and UV irradiation for 12 h, showed a significant increase (Figure 2f,h), indicating enhanced cross-linking reactions.[51,94] The AImod of the aged DOM expanded toward two opposite directions (Figure 4d), while the mean AImod for all aging processes excluding UV irradiation for 12 h consistently decreased, suggesting less carbon recalcitrance.[76] This trend aligned with changes in DBE-O. It is noteworthy that heating and UV irradiation generated a proportion of DOM substances with extreme values of high O/C, low H/C, high NOSC, and high AImod, representing the most oxidized yet recalcitrant substances[74,76,97] (Figure 4). Plausible structures of DOM substances with the highest relative abundances following various aging processes were identified, consisting of both plastic additives and degradation products containing oxidized PE oligomers (Tables S6−S13).

3.5. Implications and Limitations. Our findings offer novel insights into polymer aging dynamics, indicating that significant quantities of MPs and DOM substances can be released during the everyday use and storage of LDPE food wraps. We observed an exponential correlation between Young's modulus and the quantity of generated MPs, suggesting that a substantial number of MPs were generated in tandem with a decline in mechanical properties. Notably, a sharp reduction in mechanical properties occurred along with a substantial generation of MPs, even during the initial stages of aging. For example, only 2 min of microwave irradiation, 30 min of heating at 48 °C, 5 min of steaming, or 7 days of refrigeration resulted in the generation of 103−232 MPs/cm^2 of food wrap. Furthermore, we observed that subjecting plastic food wrap to 12 h of UV irradiation, which equates to 8.8 days of sunlight exposure, resulted in the highest generation of MPs, reaching 2034 items/cm^2. It is important to note that although no apparent surface oxidation occurred for the remaining plastic film under most aging processes, the DOM fraction released under these treatments exhibited significant oxidation characteristics. This resulted in the generation of molecules with higher oxidation, polarity, and carbon saturation even at the initial stage of aging. Such findings suggest that DOM substances showed a decoupled change in chemical properties compared with the bulk plastic film.

The significant increase in MP generation from the food wrap during everyday use and storage activities, such as heating, steaming, microwave irradiation, refrigeration, freezing, and freeze−thaw cycling, highlights a potential pathway of exposure of MPs to human beings. The substantial release of DOM also points out that such conditions are possible and non-negligible sources of submicron-sized organic substances, raising further concerns about their toxicity to organisms. Consisting of a mixture of plastic additives, oxidized PE oligomers, and other degradation products, plastic-derived DOM substances found in this study are highly oxidized and much smaller compared to bulk plastic film and MPs. Prior evidence has shown that MPs and NPs with sizes smaller than 10 μm are able to accumulate in human tissues following intestinal absorption.[18,98] The size of DOM substances investigated in this study (<0.45 μm) was much lower than this cutoff value, suggesting higher bioavailability and a greater likelihood of accumulation in cells compared to MPs. The molecular weights of DOM (200−800 Da) fell within the "oligomer" range when normalized by the PE structure, which were more bioavailable compared with MPs or NPs.[12,31] Previous studies using PS particles within the DOM size range have indeed shown that particles of this size can penetrate human and aquatic organism cells and induce toxicity, shedding light on plastic-derived DOM toxicity to organisms. For example, PS within the DOM size range is known to induce cytotoxicity, the production of reactive oxygen species, and (pro-)inflammation in human cells.[99,100] Such particles have also been reported to accumulate in the gut of zebrafish, triggering developmental toxicity, reproductive toxicity, neurotoxicity, immunotoxicity, and genotoxicity.[101,102]

Additionally, aged plastic films released oxidized DOM with a higher polarity (Section 3.4), which may account for their higher bioavailability to organisms once they enter aquatic environments, compared to those derived from pristine plastic films.[103,104] The DBE values for certain treatments, such as heating at 100 °C and UV irradiation for 12 h, were higher than those of pristine plastic film (Table S14), potentially leading to higher acute toxicity to microorganisms, as shown in previous studies.[105,106] It is also important to note that while most DOM exhibited less recalcitrance (indicating higher biodegradability), those released after heating at 100 °C and UV irradiation for 12 h had higher recalcitrance (Table S14), suggesting "heat-stabilization" and "photostabilization" processes. This aging-induced stabilization of DOM is also observed in deep ocean environments and subsoils, contributing to long-term carbon storage.[107,108] However, considering that the plastic-derived DOM from heating and UV irradiation contained toxic additives like diethyl phthalate, sucrose, dibutyl tartrate, tetraethylene glycol dimethacrylate, and triisopentyl citrate (Tables S9 and S12), the increased carbon stability of the DOM pool may also lead to prolonged exposure and toxicity to aquatic organisms. In summary, our understanding of human health and ecological risks associated with plastic-derived DOM substances is still very limited. This study provides molecular-level insights into the complex nature of plastic-derived DOM, which represents a "first step" in understanding their risks. Future studies should continue to explore the toxicity of plastic-derived DOM substances to aquatic organisms and human cells.

Given the widespread use of LDPE food wraps, establishing new guidelines for public health and safety concerns is imperative. The creation of such guidelines should include reconsidering the "microwave-safe" label for products, avoiding the preparation of food covered in plastic wrap in hot water and steamers, and rinsing the surface of food to eliminate MPs

https://doi.org/10.1021/acs.est.4c05504
Environ. Sci. Technol. XXXX, XXX, XXX−XXX

and associated submicrometer-sized DOM substances after it has been stored in refrigerators. The rapid MP generation kinetics and the highest number of DOM substances observed during UV irradiation also indicate that food wraps should ideally be stored in areas away from direct sunlight.

Finally, it should be acknowledged that some methodological challenges and limitations associated with plastic-derived DOM characterization still exist. First, the method can only accurately detect molecules containing O; therefore, unoxidized PE oligomers are not captured in this study. Additionally, the molecular weight that can be precisely characterized usually falls within 200−800 Da for FT-ICR-MS; thus, any molecules <200 or >800 Da were not included. Besides, analytes containing nitrogen (N) or sulfur (S) were not considered during FT-ICR-MS data processing, aiming to minimize the error in analyte identification, because the bulk analysis of the LDPE film did not detectthese elements; and as a result, some N- and S-containing additives in trace quantities may not be considered. It is also important to note that structural isomers cannot be distinguished using FT-ICR-MS; as a result, the proposed structures of the DOM represent a "more likely" scenario in the context of PE degradation and chemicals associated with plastic packaging.

■ ASSOCIATED CONTENT

Supporting Information

The Supporting Information is available free of charge at https://pubs.acs.org/doi/10.1021/acs.est.4c05504.

Text S1, conditional fragmentation modeling of the size distribution of MPs; Text S2, MP generation kinetics modeling; Text S3, literature search methodology; Text S4, 2D-COS analysis; Text S5, meanings of key parameters from GPC analysis; Text S6, detailed information on FT-ICR-MS data interpretation; Text S7, quality control measures and statistical analyses; Tables S1 and S2, conditional fragmentation modeling parameters and exponential modeling parameters for different aging treatments; Table S3, calculated fragmentation dimension values; Table S4, MP counting results in procedural blank samples; Table S5, analyte characteristics of shared 40 DOM substances for all groups; Tables S6−S13, analyte characteristics of the most abundant DOM substances following different aging processes; Table S14, summary of the DOM characteristics determined by FT-ICR-MS; Figure S1, conditional fragmentation modeling of the size distribution of MP generated following different aging processes; Figure S2, flow diagram reporting the number of retrieved studies; Figure S3, effect of air-drying on MP quantification; Figure S4, MP generation from large pieces of food wrap as compared with cut pieces; Figure S5, MP generation from food wrap in contact with different liquids; Figure S6, exponential fitting of MP generation characteristics; Figure S7, morphologies of the aged food wrap and the generated MP; Figure S8, FTIR spectra of the remaining plastic film following different aging treatments; Figure S9, 2D-COS maps showing the changes in surface functionality of the remaining plastic film; Figure S10, Raman spectra of the remaining plastic film following different aging treatments; Figure S11, XPS survey spectra of the remaining plastic film following different aging treatments; Figure S12, XPS C 1s spectra of the pristine and aged plastic film following microwave irradiation, heating, and steaming; Figure S13, XPS C 1s spectra of the aged plastic film following UV irradiation, refrigeration, freezing, and freeze−thaw cycling; Figure S14, correlation of DOC content with the number of FT-ICR-MS identified analytes; and Figure S15, Venn diagram showing the number of shared and unique analytes determined by FT-ICR-MS (PDF)

■ AUTHOR INFORMATION

Corresponding Author

Deyi Hou − *School of Environment, Tsinghua University, Beijing 100084, China;* orcid.org/0000-0002-0511-5806; Email: houdeyi@tsinghua.edu.cn

Authors

Liuwei Wang − *School of Environment, Tsinghua University, Beijing 100084, China;* orcid.org/0000-0002-6176-6056

Jing Gao − *School of Environment, Tsinghua University, Beijing 100084, China*

Wei-Min Wu − *Department of Civil and Environmental Engineering, William & Cloy Codiga Resource Recovery Center, Stanford University, Stanford, California 94305-4020, United States*

Jian Luo − *School of Civil and Environmental Engineering, Georgia Institute of Technology, Atlanta, Georgia 30332-0355, United States*

Michael S. Bank − *Institute of Marine Research, Bergen NO-5817, Norway;* orcid.org/0000-0001-5194-7171

Albert A. Koelmans − *Aquatic Ecology and Water Quality Management Group, Wageningen University and Research, 6700 AA Wageningen, Netherlands;* orcid.org/0000-0001-7176-4356

John J. Boland − *AMBER Research Centre and Centre for Research on Adaptive Nanostructures and Nanodevices (CRANN) and School of Chemistry, Trinity College Dublin, Dublin 2, Ireland;* orcid.org/0000-0002-3229-8038

Complete contact information is available at: https://pubs.acs.org/10.1021/acs.est.4c05504

Notes

The authors declare no competing financial interest.

■ ACKNOWLEDGMENTS

This work was supported by the National Natural Science Foundation of China (Grant No. 42225703).

■ REFERENCES

(1) *PlasticsEurope Plastics—The facts 2023*; PlasticsEurope, 2023.

(2) Yates, J.; Deeney, M.; Rolker, H. B.; White, H.; Kalamatianou, S.; Kadiyala, S. A systematic scoping review of environmental, food security and health impacts of food system plastics. *Nat. Food.* **2021**, *2* (2), 80−87.

(3) Sewwandi, M.; Wijesekara, H.; Rajapaksha, A. U.; Soysa, S.; Vithanage, M. Microplastics and plastics-associated contaminants in food and beverages; Global trends, concentrations, and human exposure. *Environ. Pollut.* **2023**, *317*, No. 120747.

(4) UNEP, *Single-use supermarket food packaging and its alternatives: Recommendations from life cycle Assessments*; United Nations Environment Programme: Nairobi, Kenya, 2022.

(5) Stevens, S.; McPartland, M.; Bartosova, Z.; Skåland, H. S.; Völker, J.; Wagner, M. Plastic Food Packaging from Five Countries

Contains Endocrine- and Metabolism-Disrupting Chemicals. *Environ. Sci. Technol.* **2024**, *58* (11), 4859−4871.
(6) Li, D.; Shi, Y.; Yang, L.; Xiao, L.; Kehoe, D. K.; Gunko, Y. K.; Boland, J. J.; Wang, J. J. Microplastic release from the degradation of polypropylene feeding bottles during infant formula preparation. *Nat. Food.* **2020**, *1* (11), 746−754.
(7) Álvarez-Fernández, C.; Matikainen, E.; McGuigan, K. G.; Andrade, J. M.; Marugán, J. Evaluation of microplastics release from solar water disinfection poly(ethylene terephthalate) and polypropylene containers. *J. Hazard. Mater.* **2024**, *465*, No. 133179.
(8) WRAP; *Creating a Circular Economy for Flexible Plastic Packaging*; The Waste and Resources Action Programme: Banbury, UK, 2021.
(9) Muncke, J.; Andersson, A. M.; Backhaus, T.; Belcher, S. M.; Boucher, J. M.; Carney Almroth, B.; Collins, T. J.; Geueke, B.; Groh, K. J.; Heindel, J. J.; von Hippel, F. A.; Legler, J.; Maffini, M. V.; Martin, O. V.; Peterson Myers, J.; Nadal, A.; Nerin, C.; Soto, A. M.; Trasande, L.; Vandenberg, L. N.; Wagner, M.; Zimmermann, L.; Thomas Zoeller, R.; Scheringer, M. A vision for safer food contact materials: Public health concerns as drivers for improved testing. *Environ. Int.* **2023**, *180*, No. 108161.
(10) WHO; *Dietary and Inhalation Exposure to Nano- and Microplastic Particles and Potential Implications for Human Health*; World Health Organization: Geneva, Switzerland, 2022.
(11) Kadac-Czapska, K.; Knez, E.; Grembecka, M. Food and human safety: the impact of microplastics. *Crit. Rev. Food Sci. Nutr.* **2024**, *64* (11), 3502−3521.
(12) MacLeod, M.; Arp, H. P. H.; Tekman, M. B.; Jahnke, A. The global threat from plastic pollution. *Science* **2021**, *373* (6550), 61−65.
(13) Espiritu, E. Q.; Pauco, J. L. R.; Bareo, R. S.; Palaypayon, G. B.; Capistrano, H. A. M.; Jabar, S. R.; Coronel, A. S. O.; Rodolfo, R. S.; Enriquez, E. P. Microplastics contamination in selected staple consumer food products. *J. Food Sci. Technol.* **2024**, *61*, 2082.
(14) Liu, L.; Zhang, X.; Jia, P.; He, S.; Dai, H.; Deng, S.; Han, J. Release of microplastics from breastmilk storage bags and assessment of intake by infants: A preliminary study. *Environ. Pollut.* **2023**, *323*, No. 121197.
(15) Hernandez, L. M.; Xu, E. G.; Larsson, H. C. E.; Tahara, R.; Maisuria, V. B.; Tufenkji, N. Plastic Teabags Release Billions of Microparticles and Nanoparticles into Tea. *Environ. Sci. Technol.* **2019**, *53* (21), 12300−12310.
(16) Vega-Herrera, A.; Garcia-Torné, M.; Borrell-Diaz, X.; Abad, E.; Llorca, M.; Villanueva, C. M.; Farré, M. Exposure to micro(nano)-plastics polymers in water stored in single-use plastic bottles. *Chemosphere* **2023**, *343*, No. 140106.
(17) Hussain, K. A.; Romanova, S.; Okur, I.; Zhang, D.; Kuebler, J.; Huang, X.; Wang, B.; Fernandez-Ballester, L.; Lu, Y.; Schubert, M.; Li, Y. Assessing the Release of Microplastics and Nanoplastics from Plastic Containers and Reusable Food Pouches: Implications for Human Health. *Environ. Sci. Technol.* **2023**, *57* (26), 9782−9792.
(18) Mohamed Nor, N. H.; Kooi, M.; Diepens, N. J.; Koelmans, A. A. Lifetime Accumulation of Microplastic in Children and Adults. *Environ. Sci. Technol.* **2021**, *55* (8), 5084−5096.
(19) Wang, F.; Xiang, L.; Sze-Yin Leung, K.; Elsner, M.; Zhang, Y.; Guo, Y.; Pan, B.; Sun, H.; An, T.; Ying, G.; Brooks, B. W.; Hou, D.; Helbling, D. E.; Sun, J.; Qiu, H.; Vogel, T. M.; Zhang, W.; Gao, Y.; Simpson, M. J.; Luo, Y.; Chang, S. X.; Su, G.; Wong, B. M.; Fu, T.-M.; Zhu, D.; Jobst, K. J.; Ge, C.; Coulon, F.; Harindintwali, J. D.; Zeng, X.; Wang, H.; Fu, Y.; Wei, Z.; Lohmann, R.; Chen, C.; Song, Y.; Sanchez-Cid, C.; Wang, Y.; El-Naggar, A.; Yao, Y.; Huang, Y.; Cheuk-Fung Law, J.; Gu, C.; Shen, H.; Gao, Y.; Qin, C.; Li, H.; Zhang, T.; Corcoll, N.; Liu, M.; Alessi, D. S.; Li, H.; Brandt, K. K.; Pico, Y.; Gu, C.; Guo, J.; Su, J.; Corvini, P.; Ye, M.; Rocha-Santos, T.; He, H.; Yang, Y.; Tong, M.; Zhang, W.; Suanon, F.; Brahushi, F.; Wang, Z.; Hashsham, S. A.; Virta, M.; Yuan, Q.; Jiang, G.; Tremblay, L. A.; Bu, Q.; Wu, J.; Peijnenburg, W.; Topp, E.; Cao, X.; Jiang, X.; Zheng, M.; Zhang, T.; Luo, Y.; Zhu, L.; Li, X.; Barceló, D.; Chen, J.; Xing, B.; Amelung, W.; Cai, Z.; Naidu, R.; Shen, Q.; Pawliszyn, J.; Zhu, Y.-G.; Schaeffer, A.; Rillig, M. C.; Wu, F.; Yu, G.; Tiedje, J. M. Emerging contaminants: A One Health perspective. *Innovation* **2024**, *5* (4), No. 100612.
(20) Nguyen, M.-K.; Rakib, M. R. J.; Lin, C.; Hung, N. T. Q.; Le, V.-G.; Nguyen, H.-L.; Malafaia, G.; Idris, A. M. A comprehensive review on ecological effects of microplastic pollution: An interaction with pollutants in the ecosystems and future perspectives. *Trac-trend. Anal. Chem.* **2023**, *168*, No. 117294.
(21) Qian, N.; Gao, X.; Lang, X.; Deng, H.; Bratu, T. M.; Chen, Q.; Stapleton, P.; Yan, B.; Min, W. Rapid single-particle chemical imaging of nanoplastics by SRS microscopy. *Proc. Natl. Acad. Sci. U. S. A.* **2024**, *121* (3), No. e2300582121.
(22) Abdolahpur Monikh, F.; Baun, A.; Hartmann, N. B.; Kortet, R.; Akkanen, J.; Lee, J.-S.; Shi, H.; Lahive, E.; Uurasjärvi, E.; Tufenkji, N.; Altmann, K.; Wiesner, Y.; Grossart, H.-P.; Peijnenburg, W.; Kukkonen, J. V. K. Exposure protocol for ecotoxicity testing of microplastics and nanoplastics. *Nat. Protoc.* **2023**, *18* (11), 3534−3564.
(23) Son, J.-W.; Nam, Y.; Kim, C. Nanoplastics from disposable paper cups and microwavable food containers. *J. Hazard. Mater.* **2024**, *464*, No. 133014.
(24) Fang, C.; Luo, Y.; Naidu, R. Microplastics and nanoplastics analysis: Options, imaging, advancements and challenges. *Trac-trend. Anal. Chem.* **2023**, *166*, No. 117158.
(25) Choi, S.; Lee, S.; Kim, M.-K.; Yu, E.-S.; Ryu, Y.-S. Challenges and Recent Analytical Advances in Micro/Nanoplastic Detection. *Anal. Chem.* **2024**, *96*, 8846−8854.
(26) Pei, W.; Hu, R.; Liu, H.; Wang, L.; Lai, Y. Advanced Raman spectroscopy for nanoplastics analysis: Progress and perspective. *Trac-trend. Anal. Chem.* **2023**, *166*, No. 117188.
(27) Wlasits, P. J.; Konrat, R.; Winkler, P. M. Heterogeneous Nucleation of Supersaturated Water Vapor onto Sub-10 nm Nanoplastic Particles. *Environ. Sci. Technol.* **2023**, *57* (4), 1584−1591.
(28) Abi Farraj, S.; Lapointe, M.; Kurusu, R. S.; Liu, Z.; Barbeau, B.; Tufenkji, N. Targeting nanoplastic and microplastic removal in treated wastewater with a simple indicator. *Nat. Water* **2024**, *2* (1), 72−83.
(29) Zhao, J.; Lan, R.; Wang, Z.; Su, W.; Song, D.; Xue, R.; Liu, Z.; Liu, X.; Dai, Y.; Yue, T.; Xing, B. Microplastic fragmentation by rotifers in aquatic ecosystems contributes to global nanoplastic pollution. *Nat. Nanotechnol.* **2024**, *19* (3), 406−414.
(30) Yang, T.; Xu, Y.; Liu, G.; Nowack, B. Oligomers are a major fraction of the submicrometre particles released during washing of polyester textiles. *Nat. Water* **2024**, *2* (2), 151−160.
(31) Shi, C.; Wang, M.; Wang, Z.; Qu, G.; Jiang, W.; Pan, X.; Fang, M. Oligomers from the Synthetic Polymers: Another Potential Iceberg of New Pollutants. *Environ. Health* **2023**, *1* (4), 228−235.
(32) Nerín, C.; Canellas, E.; Vera, P., *Migration of packaging and labeling components and advances in analytical methodology supporting exposure assessment*. In Present Knowledge in Food Safety, Knowles, M. E.; Anelich, L. E.; Boobis, A. R.; Popping, B., Eds. Academic Press: 2023; pp 218−239.
(33) Pelegrini, K.; Pereira, T. C. B.; Maraschin, T. G.; Teodoro, L. D. S.; Basso, N. R. D. S.; De Galland, G. L. B.; Ligabue, R. A.; Bogo, M. R. Micro- and nanoplastic toxicity: A review on size, type, source, and test-organism implications. *Sci. Total Environ.* **2023**, *878*, No. 162954.
(34) Cui, Q.; Wang, F.; Wang, X.; Chen, T.; Guo, X. Environmental toxicity and ecological effects of micro(nano)plastics: A huge challenge posed by biodegradability. *Trac-trend. Anal. Chem.* **2023**, *164*, No. 117092.
(35) Gong, H.; Li, R.; Li, F.; Guo, X.; Xu, L.; Gan, L.; Yan, M.; Wang, J. Toxicity of nanoplastics to aquatic organisms: Genotoxicity, cytotoxicity, individual level and beyond individual level. *J. Hazard. Mater.* **2023**, *443*, No. 130266.
(36) Romera-Castillo, C.; Pinto, M.; Langer, T. M.; Álvarez-Salgado, X. A.; Herndl, G. J. Dissolved organic carbon leaching from plastics stimulates microbial activity in the ocean. *Nat. Commun.* **2018**, *9* (1), 1430.

https://doi.org/10.1021/acs.est.4c05504
Environ. Sci. Technol. XXXX, XXX, XXX−XXX

(37) Stubbins, A.; Zhu, L.; Zhao, S.; Spencer, R. G. M.; Podgorski, D. C. Molecular Signatures of Dissolved Organic Matter Generated from the Photodissolution of Microplastics in Sunlit Seawater. *Environ. Sci. Technol.* **2023**, *57* (48), 20097−20106.
(38) Liu, S.; Qiu, Y.; He, Z.; Shi, C.; Xing, B.; Wu, F. Microplastic-derived dissolved organic matter and its biogeochemical behaviors in aquatic environments: A review. *Crit. Rev. Environ. Sci. Technol.* **2024**, *54* (11), 865−882.
(39) Lee, Y. K.; Romera-Castillo, C.; Hong, S.; Hur, J. Characteristics of microplastic polymer-derived dissolved organic matter and its potential as a disinfection byproduct precursor. *Water Res.* **2020**, *175*, No. 115678.
(40) Lee, Y. K.; Murphy, K. R.; Hur, J. Fluorescence Signatures of Dissolved Organic Matter Leached from Microplastics: Polymers and Additives. *Environ. Sci. Technol.* **2020**, *54* (19), 11905−11914.
(41) Romera-Castillo, C.; Birnstiel, S.; Álvarez-Salgado, X. A.; Sebastián, M. Aged Plastic Leaching of Dissolved Organic Matter Is Two Orders of Magnitude Higher Than Virgin Plastic Leading to a Strong Uplift in Marine Microbial Activity. *Front. Mar. Sci.* **2022**, *9*, No. 861557.
(42) Zhou, P.; Tian, L.; Siddique, M. S.; Song, S.; Graham, N. J. D.; Zhu, Y.-G.; Yu, W. Divergent Fate and Roles of Dissolved Organic Matter from Spatially Varied Grassland Soils in China During Long-Term Biogeochemical Processes. *Environ. Sci. Technol.* **2024**, *58* (2), 1164−1176.
(43) Hermes, A. L.; Logan, M. N.; Poulin, B. A.; McKenna, A. M.; Dawson, T. E.; Borch, T.; Hinckley, E.-L. S. Agricultural Sulfur Applications Alter the Quantity and Composition of Dissolved Organic Matter from Field-to-Watershed Scales. *Environ. Sci. Technol.* **2023**, *57* (27), 10019−10029.
(44) Xu, Y.; Wang, X.; Ou, Q.; Zhou, Z.; van der Hoek, J. P.; Liu, G. Appearance of Recalcitrant Dissolved Black Carbon and Dissolved Organic Sulfur in River Waters Following Wildfire Events. *Environ. Sci. Technol.* **2024**, *58* (16), 7165−7175.
(45) Ruan, M.; Wu, F.; Sun, F.; Song, F.; Li, T.; He, C.; Jiang, J. Molecular-level exploration of properties of dissolved organic matter in natural and engineered water systems: A critical review of FTICR-MS application. *Crit. Rev. Environ. Sci. Technol.* **2023**, *53* (16), 1534−1562.
(46) Qi, Y.; Xie, Q.; Wang, J.-J.; He, D.; Bao, H.; Fu, Q.-L.; Su, S.; Sheng, M.; Li, S.-L.; Volmer, D. A.; Wu, F.; Jiang, G.; Liu, C.-Q.; Fu, P. Deciphering dissolved organic matter by Fourier transform ion cyclotron resonance mass spectrometry (FT-ICR MS): from bulk to fractions and individuals. *Carbon Res.* **2022**, *1* (1), 3.
(47) Lee, Y. K.; He, W.; Guo, H.; Karanfil, T.; Hur, J. Effects of organic additives on spectroscopic and molecular-level features of photo-induced dissolved organic matter from microplastics. *Water Res.* **2023**, *242*, No. 120272.
(48) Zhang, J.; Hou, X.; Zhang, K.; Deng, Y.; Xiao, Q.; Gao, Y.; Zhou, X.; Yan, B. Deciphering fluorescent and molecular fingerprint of dissolved organic matter leached from microplastics in water. *Water Res.* **2024**, *250*, No. 121047.
(49) Song, F.; Li, T.; Hur, J.; Shi, Q.; Wu, F.; He, W.; Shi, D.; He, C.; Zhou, L.; Ruan, M.; Cao, Y. Molecular-level insights into the heterogeneous variations and dynamic formation mechanism of leached dissolved organic matter during the photoaging of polystyrene microplastics. *Water Res.* **2023**, *242*, No. 120114.
(50) ISO ISO 4892-3:2016; *Plastics—Methods of Exposure to Laboratory Light Sources—Part 3: Fluorescent UV Lamps*; International Organization for Standardization, 2016.
(51) Grause, G.; Chien, M. F.; Inoue, C. Changes during the weathering of polyolefins. *Polym. Degrad. Stab.* **2020**, *181*, No. 109364.
(52) Gao, J.; Wang, L.; Wu, W. M.; Luo, J.; Hou, D. Microplastic generation from field-collected plastic gauze: Unveiling the aging processes. *J. Hazard. Mater.* **2024**, *466*, No. 133615.
(53) Wang, L.; Guo, J.; Bank, M. S.; Van Zwieten, L.; Bolan, N. S.; Wu, W. M.; Hou, D. Organo-mineral interaction between plastic film and sedimentary rock induced by UV irradiation. *Chem. Geol.* **2024**, *662*, No. 122240.
(54) Liu, H.; Hu, B.; Zhang, L.; Zhao, X. J.; Shang, K. Z.; Wang, Y. S.; Wang, J. Ultraviolet radiation over China: Spatial distribution and trends. *Renew. Sust. Energy Rev.* **2017**, *76*, 1371−1383.
(55) US FDA Guidance for Industry; *Preparation of Premarket Submissions for Food Contact Substances (Chemistry Recommendations)*; United States Food and Drug Administration: New Hampshire Ave, Silver Spring, 2007.
(56) Maes, T.; Jessop, R.; Wellner, N.; Haupt, K.; Mayes, A. G. A rapid-screening approach to detect and quantify microplastics based on fluorescent tagging with Nile Red. *Sci. Rep.* **2017**, *7* (1), 44501.
(57) Wang, L.; Li, P.; Zhang, Q.; Wu, W. M.; Luo, J.; Hou, D. Modeling the Conditional Fragmentation-Induced Microplastic Distribution. *Environ. Sci. Technol.* **2021**, *55* (9), 6012−6021.
(58) Di Pippo, F.; Venezia, C.; Sighicelli, M.; Pietrelli, L.; Di Vito, S.; Nuglio, S.; Rossetti, S. Microplastic-associated biofilms in lentic Italian ecosystems. *Water Res.* **2020**, *187*, No. 116429.
(59) Maxwell, S. H.; Melinda, K. F.; Matthew, G. Counterstaining to separate Nile red-stained microplastic particles from terrestrial invertebrate biomass. *Environ. Sci. Technol.* **2020**, *54* (9), 5580−5588.
(60) Rosal, R. Morphological description of microplastic particles for environmental fate studies. *Mar. Pollut. Bull.* **2021**, *171*, No. 112716.
(61) Cole, M.; Galloway, T. S. Ingestion of nanoplastics and microplastics by Pacific oyster larvae. *Environ. Sci. Technol.* **2015**, *49* (24), 14625−14632.
(62) Ghabezi, P.; Harrison, N. M. Indentation characterization of glass/epoxy and carbon/epoxy composite samples aged in artificial salt water at elevated temperature. *Polym. Test.* **2022**, *110*, No. 107588.
(63) O'Carroll, A.; Hardiman, M.; Tobin, E. F.; Young, T. M. Correlation of the rain erosion performance of polymers to mechanical and surface properties measured using nanoindentation. *Wear* **2018**, *412*−*413*, 38−48.
(64) Noda, I.; Ozaki, Y. *Two-Dimensional Correlation Spectroscopy: Applications in Vibrational and Optical Spectroscopy*; John Wiley & Sons: 2005.
(65) Greczynski, G.; Haasch, R. T.; Hellgren, N.; Lewin, E.; Hultman, L. X-ray Photoelectron Spectroscopy of Thin Films. *Nat. Rev. Method. Prim.* **2023**, *3* (1), 40.
(66) Li, D.; Sheerin, E. D.; Shi, Y.; Xiao, L.; Yang, L.; Boland, J. J.; Wang, J. J. Alcohol Pretreatment to Eliminate the Interference of Micro Additive Particles in the Identification of Microplastics Using Raman Spectroscopy. *Environ. Sci. Technol.* **2022**, *56* (17), 12158−12168.
(67) Xie, L.; Luo, S.; Liu, Y.; Ruan, X.; Gong, K.; Ge, Q.; Li, K.; Valev, V. K.; Liu, G.; Zhang, L. Automatic Identification of Individual Nanoplastics by Raman Spectroscopy Based on Machine Learning. *Environ. Sci. Technol.* **2023**, *57* (46), 18203−18214.
(68) Sanluis-Verdes, A.; Colomer-Vidal, P.; Rodriguez-Ventura, F.; Bello-Villarino, M.; Spinola-Amilibia, M.; Ruiz-Lopez, E.; Illanes-Vicioso, R.; Castroviejo, P.; Aiese Cigliano, R.; Montoya, M.; Falabella, P.; Pesquera, C.; Gonzalez-Legarreta, L.; Arias-Palomo, E.; Solà, M.; Torroba, T.; Arias, C. F.; Bertocchini, F. Wax worm saliva and the enzymes therein are the key to polyethylene degradation by Galleria mellonella. *Nat. Commun.* **2022**, *13* (1), 5568.
(69) Tennakoon, A.; Wu, X.; Paterson, A. L.; Patnaik, S.; Pei, Y.; LaPointe, A. M.; Ammal, S. C.; Hackler, R. A.; Heyden, A.; Slowing, I. I.; Coates, G. W.; Delferro, M.; Peters, B.; Huang, W.; Sadow, A. D.; Perras, F. A. Catalytic upcycling of high-density polyethylene via a processive mechanism. *Nat. Catal.* **2020**, *3* (11), 893−901.
(70) Cao, R.; Zhang, M. Q.; Hu, C.; Xiao, D.; Wang, M.; Ma, D. Catalytic oxidation of polystyrene to aromatic oxygenates over a graphitic carbon nitride catalyst. *Nat. Commun.* **2022**, *13* (1), 4809.
(71) Kong, D.; Wang, L.; Chen, X.; Xia, W.; Su, L.; Zuo, F.; Yan, Z.; Chen, S.; Wu, J. Chemical-biological degradation of polyethylene combining Baeyer-Villiger oxidation and hydrolysis reaction of cutinase. *Green Chem.* **2022**, *24* (5), 2203−2211.

https://doi.org/10.1021/acs.est.4c05504
Environ. Sci. Technol. XXXX, XXX, XXX−XXX

(72) Peng, B. Y.; Sun, Y.; Wu, Z.; Chen, J.; Shen, Z.; Zhou, X.; Wu, W. M.; Zhang, Y. Biodegradation of polystyrene and low-density polyethylene by Zophobas atratus larvae: Fragmentation into microplastics, gut microbiota shift, and microbial functional enzymes. *J. Clean. Prod.* **2022**, *367*, No. 132987.
(73) Zhang, Q.; Lv, J.; He, A.; Cao, D.; He, X.; Zhao, L.; Wang, Y.; Jiang, G. Investigation with ESI FT-ICR MS on sorbent selectivity and comprehensive molecular composition of landfill leachate dissolved organic matter. *Water Res.* **2023**, *243*, No. 120359.
(74) Kellerman, A. M.; Kothawala, D. N.; Dittmar, T.; Tranvik, L. J. Persistence of dissolved organic matter in lakes related to its molecular characteristics. *Nat. Geosci.* **2015**, *8* (6), 454−457.
(75) Jennings, E.; Kremser, A.; Han, L.; Reemtsma, T.; Lechtenfeld, O. J. Discovery of Polar Ozonation Byproducts via Direct Injection of Effluent Organic Matter with Online LC-FT-ICR-MS. *Environ. Sci. Technol.* **2022**, *56* (3), 1894−1904.
(76) Koch, B. P.; Dittmar, T. From mass to structure: an aromaticity index for high-resolution mass data of natural organic matter. *Rapid Commun. Mass Sp.* **2006**, *20* (5), 926−932.
(77) Groh, K. J.; Backhaus, T.; Carney-Almroth, B.; Geueke, B.; Inostroza, P. A.; Lennquist, A.; Leslie, H. A.; Maffini, M.; Slunge, D.; Trasande, L.; Warhurst, A. M.; Muncke, J. Overview of known plastic packaging-associated chemicals and their hazards. *Sci. Total Environ.* **2019**, *651*, 3253−3268.
(78) *ECHA Mapping Exercise—Plastic Additives Initiative*, 2024, European Chemicals Agency: Helsinki, Finland.
(79) *Food Packaging Forum Food Contact Chemicals database (FCCdb)*. 2020, Food Packaging Forum: Zurich, Switzerland.
(80) Song, X.-C.; Canellas, E.; Dreolin, N.; Goshawk, J.; Nerin, C. A Collision Cross Section Database for extractables and Leachables from Food Contact Materials. *J. Agric. Food. Chem.* **2022**, *70* (14), 4457−4466.
(81) Huang, Q.; Cheng, Z.; Yang, C.; Wang, H.; Zhu, N.; Cao, X.; Lou, Z. Booming microplastics generation in landfill: An exponential evolution process under temporal pattern. *Water Res.* **2022**, *223*, No. 119035.
(82) Yang, Y.; Li, Z.; Yan, C.; Chadwick, D.; Jones, D. L.; Liu, E.; Liu, Q.; Bai, R.; He, W. Kinetics of microplastic generation from different types of mulch films in agricultural soil. *Sci. Total Environ.* **2022**, *814*, No. 152572.
(83) Napper, I. E.; Wright, L. S.; Barrett, A. C.; Parker-Jurd, F. N. F.; Thompson, R. C. Potential microplastic release from the maritime industry: Abrasion of rope. *Sci. Total Environ.* **2022**, *804*, No. 150155.
(84) Zhang, X.; Lin, T.; Wang, X. Investigation of microplastics release behavior from ozone-exposed plastic pipe materials. *Environ. Pollut.* **2022**, *296*, No. 118758.
(85) Efimova, I.; Bagaeva, M.; Bagaev, A.; Kileso, A.; Chubarenko, I. P. Secondary Microplastics Generation in the Sea Swash Zone with Coarse Bottom Sediments: Laboratory Experiments. *Front. Mar. Sci.* **2018**, *5*, 313.
(86) Kinloch, A. J. Micromechanisms of crack extension in polymers. *Met. Sci.* **1980**, *14* (8−9), 305−318.
(87) Liu, J.; Zhang, T.; Tian, L.; Liu, X.; Qi, Z.; Ma, Y.; Ji, R.; Chen, W. Aging Significantly Affects Mobility and Contaminant-Mobilizing Ability of Nanoplastics in Saturated Loamy Sand. *Environ. Sci. Technol.* **2019**, *53* (10), 5805−5815.
(88) Yu, Y.; Battu, A. K.; Varga, T.; Denny, A. C.; Zahid, T. M.; Chowdhury, I.; Flury, M. Minimal Impacts of Microplastics on Soil Physical Properties under Environmentally Relevant Concentrations. *Environ. Sci. Technol.* **2023**, *57* (13), 5296−5304.
(89) Hawkins, W. L. *Polymer Degradation and Stabilization*; Springer-Verlag: Berlin, Germany, 1984.
(90) Scott, G. *Mechanisms of Polymer Degradation and Stabilisation*; Elsevier: New York, USA, 1990.
(91) Roy, P. K.; Hakkarainen, M.; Varma, I. K.; Albertsson, A. C. Degradable polyethylene: Fantasy or reality. *Environ. Sci. Technol.* **2011**, *45* (10), 4217−4227.
(92) Liu, L.; Xu, M.; Ye, Y.; Zhang, B. On the degradation of (micro)plastics: Degradation methods, influencing factors, environmental impacts. *Sci. Total Environ.* **2022**, *806*, No. 151312.
(93) Pickett, J. E., *Chapter 8—Weathering of Plastics*. In Handbook of Environmental Degradation of Materials, 3rd ed.; Kutz, M., Ed.; William Andrew Publishing: 2018; pp 163−184.
(94) David, C.; Trojan, M.; Daro, A.; Demarteau, W. Photodegradation of polyethylene: comparison of various photoinitiators in natural weathering conditions. *Polym. Degrad. Stab.* **1992**, *37* (3), 233−245.
(95) Zhu, K.; Jia, H.; Zhao, S.; Xia, T.; Guo, X.; Wang, T.; Zhu, L. Formation of Environmentally Persistent Free Radicals on Microplastics under Light Irradiation. *Environ. Sci. Technol.* **2019**, *53* (14), 8177−8186.
(96) Hsueh, H.-C.; Kim, J. H.; Orski, S.; Fairbrother, A.; Jacobs, D.; Perry, L.; Hunston, D.; White, C.; Sung, L. Micro and macroscopic mechanical behaviors of high-density polyethylene under UV irradiation and temperature. *Polym. Degrad. Stab.* **2020**, *174*, No. 109098.
(97) D'Andrilli, J.; Cooper, W. T.; Foreman, C. M.; Marshall, A. G. An ultrahigh-resolution mass spectrometry index to estimate natural organic matter lability. *Rapid Commun. Mass Sp.* **2015**, *29* (24), 2385−2401.
(98) Cox, K. D.; Covernton, G. A.; Davies, H. L.; Dower, J. F.; Juanes, F.; Dudas, S. E. Human Consumption of Microplastics. *Environ. Sci. Technol.* **2019**, *53* (12), 7068−7074.
(99) Lehner, R.; Weder, C.; Petri-Fink, A.; Rothen-Rutishauser, B. Emergence of Nanoplastic in the Environment and Possible Impact on Human Health. *Environ. Sci. Technol.* **2019**, *53* (4), 1748−1765.
(100) Shi, Q.; Tang, J.; Liu, R.; Wang, L. Toxicity in vitro reveals potential impacts of microplastics and nanoplastics on human health: A review. *Crit. Rev. Environ. Sci. Technol.* **2022**, *52* (21), 3863−3895.
(101) Sendra, M.; Pereiro, P.; Yeste, M. P.; Mercado, L.; Figueras, A.; Novoa, B. Size matters: Zebrafish (Danio rerio) as a model to study toxicity of nanoplastics from cells to the whole organism. *Environ. Pollut.* **2021**, *268*, No. 115769.
(102) Bhagat, J.; Zang, L.; Nishimura, N.; Shimada, Y. Zebrafish: An emerging model to study microplastic and nanoplastic toxicity. *Sci. Total Environ.* **2020**, *728*, No. 138707.
(103) Zhang, X.; Han, J.; Zhang, X.; Shen, J.; Chen, Z.; Chu, W.; Kang, J.; Zhao, S.; Zhou, Y. Application of Fourier transform ion cyclotron resonance mass spectrometry to characterize natural organic matter. *Chemosphere* **2020**, *260*, No. 127458.
(104) LaRowe, D. E.; Van Cappellen, P. Degradation of natural organic matter: A thermodynamic analysis. *Geochim. Cosmochim. Acta* **2011**, *75* (8), 2030−2042.
(105) Han, C.; You, J.; Zhao, A.; Liao, K.; Ren, H.; Hu, H. Intermittent polarization: A promising strategy for microbial electricity driven reduction of DOM toxicity in actual industrial wastewater. *Water Res.* **2024**, *262*, No. 122099.
(106) Zhang, B.; Shan, C.; Hao, Z.; Liu, J.; Wu, B.; Pan, B. Transformation of dissolved organic matter during full-scale treatment of integrated chemical wastewater: Molecular composition correlated with spectral indexes and acute toxicity. *Water Res.* **2019**, *157*, 472−482.
(107) Hansell, D. A. Recalcitrant dissolved organic carbon fractions. *Annu. Rev. Mar. Sci.* **2013**, *5*, 421−445.
(108) Kalks, F.; Liebmann, P.; Wordell-Dietrich, P.; Guggenberger, G.; Kalbitz, K.; Mikutta, R.; Helfrich, M.; Don, A. Fate and stability of dissolved organic carbon in topsoils and subsoils under beech forests. *Biogeochemistry* **2020**, *148* (2), 111−128.

https://doi.org/10.1021/acs.est.4c05504
Environ. Sci. Technol. XXXX, XXX, XXX−XXX